Synthesis, Properties, and Catalytic Applications of Caged, Compact Trialkylphosphine 4-Phenyl-1-phospha-4-silabicyclo[2.2.2]octane

Atsuko Ochida, Go Hamasaka, Yoshihiro Yamauchi, Soichiro Kawamorita, Naoya Oshima, Kenji Hara, Hirohisa Ohmiya, and Masaya Sawamura*

Department of Chemistry, Faculty of Science, Hokkaido University, Sapporo 060-0810, Japan

Received June 20, 2008

Synthesis, properties, and catalytic applications of a caged trialkylphosphine ligand with Me_3P-like steric and electronic characters, 4-phenyl-1-phospha-4-silabicyclo[2.2.2]octane (Ph-SMAP), are reported. Given a phenyl group at the silicon atom, the Ph-SMAP ligand displayed nonvolatility with retention of Me_3P-like steric and electronic properties. The new ligand is air-stable, crystalline, and easy to handle. Single-crystal X-ray diffraction analyses of Ph-SMAP and its coordination compounds such as borane, rhodium(I), and Pt(II) complexes revealed a rigid, linear structural feature of the Ph-SMAP framework. DFT calculations [B3LYP/6-31G(d,p)] indicated that the electron-donating ability of Ph-SMAP is slightly stronger than that of Me_3P and that replacement of Si atom of Ph-SMAP with a carbon atom drastically decreases the donor power. The Ph-SMAP ligand markedly accelerated the rhodium-catalyzed hydrosilylation and hydrogenation of ketones as compared with the effect of conventional phosphine ligands such as Me_3P, Bu_3P, $(t\text{-}Bu)_3P$, and PPh_3, when it was used in combination with $[\{RhCl(C_2H_4)_2\}_2]$ and [Rh(OMe)(cod)], respectively, with P/Rh ratio of 1:1.

Introduction

Trialkylphosphines with various structures are used in coordination chemistry and organometallic chemistry as metal-coordinating ligands with strong σ-donating ability. One ligand with the extremely low steric demand is trimethylphosphine (Me_3P). We have designed and synthesized a new Me_3P-like trialkylphosphine ligand **1** (SMAP, named after *s*ilicon-constrained *m*onodentate *a*lkyl *p*hosphine) (Chart 1).[1] A new feature of this ligand is the presence of a site for functionalization at the backside of the P lone pair, which is not the case for Me_3P. The SMAP ligand **1** contains phosphorus and silicon atoms at each bridgehead of the bicyclo[2.2.2]octane framework. The molecular constraint of the bicyclic framework makes the steric demand around the phosphorus center as small as that of Me_3P and projects the P lone pair and the Si-substituent (R) in diametrically opposite directions on the straight line defined by two bridgehead atoms (see Chart 1). P-donor ligands that can be functionalized with such a directional constraint are rarely found and are limited to phosphaalkynes (**2**),[2] phosphabenzenes (**3**),[3] bicyclic phosphites (**4**),[4] phosphatriptycenes (**5**),[5] and phosphabarrelenes (**6**).[6] To the best of our knowledge, no analogous trialkylphosphine ligand exists.[7]

We previously reported preliminary results on the synthesis of the first example of SMAP (**1a**, Ph-SMAP), which contains a phenyl group on the Si atom that provides properties of high crystallinity, nonvolatility, and scentlessness.[1a] These properties arise from the rigidity of the bicyclic framework, which promotes molecular assembly into a crystal phase.

Taking advantage of the ease of the silicon-centered functionalization with the directional constraint, we further developed two classes of solid-supported SMAP ligands Silica-SMAP (**7**)[8] and [Au]-SMAP (**8**),[9] which are shown in Chart 2. In Silica-SMAP (**7**), the SMAP cages are anchored on a silica gel surface through a disiloxane bond involving the bridgehead Si atom and the surface Si atom. The immobilized phosphine showed unique coordination behavior to form a 1:1 transition metal−P complex. The heterogeneous catalyst, prepared from Silica-SMAP and $[RhCl(C_2H_4)_2]_2$, showed an exceptionally high activity for the hydrosilylation of sterically hindered ketones.[8] On the other hand, [Au]-SMAP (**8**), in a chip form, was prepared through the formation of self-assembled monolayer on a gold surface with the SMAP derivative bearing an alkanethiol pendant chain. The rhodium catalyst prepared from [Au]-SMAP (**8**) and $[RhCl(C_2H_4)_2]_2$ was used for dehydrogenative alcohol silylation and exhibited high activity and selectivity as well as highly efficient reusability.[9]

* Corresponding author. E-mail: sawamura@sci.hokudai.ac.jp.

(1) (a) Ochida, A.; Hara, K.; Ito, H.; Sawamura, M. *Org. Lett.* **2003**, *5*, 2671–2674. (b) Ochida, A.; Ito, S.; Miyahara, T.; Ito, H.; Sawamura, M. *Chem. Lett.* **2006**, *35*, 294–295.

(2) (a) Markovskii, L. N.; Romanenko, V. D. *Tetrahedron* **1989**, *45*, 6019. (b) Nixon, J. F. *Chem. Soc. Rev.* **1995**, *24*, 319–328.

(3) Le Floch, P.; Mathey, F. *Coord. Chem. Rev.* **1998**, *178−180*, 771–791.

(4) Wadsworth, W. S., Jr.; Emmons, W. D. *J. Am. Chem. Soc.* **1962**, *84*, 610–617.

(5) (a) For E = C, see: Jongsma, C.; De Kleijn, J. P.; Bickelhaupt, F. *Tetrahedron* **1974**, *30*, 3465–3469. (b) Kobayashi, J.; Agou, T.; Kawashima, T. *Chem. Lett.* **2003**, *21*, 1144–1145. (c) Agou, T.; Kobayashi, J.; Kawashima, T. *Chem. Lett.* **2004**, *33*, 1028–1029. (d) Agou, T.; Kobayashi, J.; Kawashima, T. *Heteroat. Chem.* **2004**, *15*, 437–446. (e) For *E* = Si, see: Tsuji, H.; Inoue, T.; Kaneta, Y.; Sase, S.; Kawachi, A.; Tamao, K. *Organometallics* **2006**, *25*, 6142−6148. (f) For *E* = Ge, see: Rot, N.; De Wijs, W.-J. A.; De Kanter, F. J. J.; Dam, M. A.; Bickelhaupt, F.; Lutz, M.; Spek, A. L. *Main Group Met. Chem.* **1999**, *22*, 519–526.

(6) (a) Breit, B.; Fuchs, E. *Chem. Comm.* **2004**, 694–695. (b) Fuchs, E.; Manfred Keller, M.; Breit, B. *Chem. Eur. J.* **2006**, *12*, 6930–6939.

(7) (a) For a diphosphine with a related structure, 1,4-diphosphabicyclo[2.2.2]octane, see: Hinton, R. C.; Mann, F. G. *J. Chem. Soc.* **1959**, 2835. (b) See also: Thirupathi, N.; Stricklen, P. M.; Liu, X.; Oshel, R.; Guzei, I.; Ellern, A.; Verkade, J. G. *Inorg. Chem.* **2007**, *46*, 9351–9363.

(8) Hamasaka, G.; Ochida, A.; Hara, K.; Sawamura, M. *Angew. Chem., Int. Ed.* **2007**, *46*, 5381–5383.

(9) Hara, K.; Akiyama, R.; Takakusagi, S.; Uosaki, K.; Yoshino, T.; Kagi, H.; Sawamura, M. *Angew. Chem., Int. Ed.* **2008**, *47*, 5627–5630.

10.1021/om8005728 CCC: $40.75
Publication on Web 10/01/2008

Chart 1. Structures of SMAP and Related P-Donor Ligands

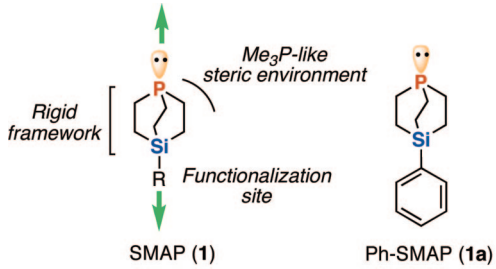

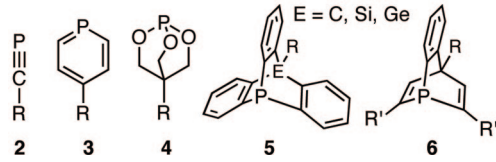

Chart 2. Solid-Supported SMAP Ligands

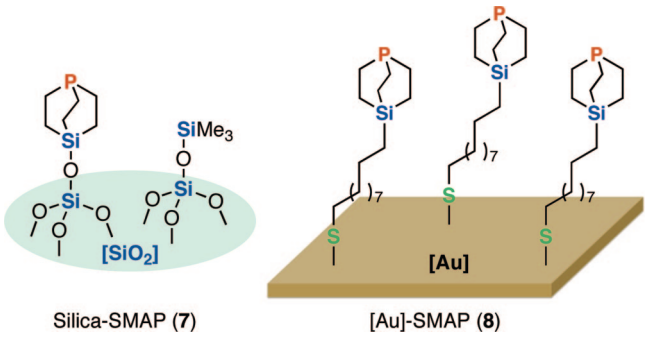

This article reports details of our studies on the synthesis and properties of Ph-SMAP (**1**), the parent compound for various SMAP-type compounds, and some results on its applications as a soluble ligand for homogeneous transition metal catalysis.

Results and Discussion

Synthesis. In numerous studies pursuing the efficient synthesis of Ph-SMAP, we have developed a route that uses benzylphosphine (**11**) as a source of the P atom of Ph-SMAP as shown in Scheme 1. As compared with the previously reported synthesis,[1a] which used phenylphosphine, the new route is more expeditious and features higher total yield. Thus, phenyltrivinylsilane (**9**),[10] which was prepared from $PhSiCl_3$ and vinylmagnesium bromide in 85% yield, was converted into tribromide **10** in 88% yield (recrystallization) through *anti*-Markovnikov HBr addition. On the other hand, benzylphosphine (**11**)[11] was prepared from diethyl benzylphosphonate (prepared from benzyl bromide and triethyl phosphite) in 66% yield through $LiAlH_4$ reduction in the presence of Me_3SiCl. Benzylphosphine (**11**) was treated with BH_3·THF to convert into a borane complex. The in-situ-prepared phosphine−borane complex was subjected to 2-fold P-alkylation with 2 equiv of tribromide **10** in the presence of sodium hydride to give monocyclic phosphine−borane **12** in 71% yield based on **11** (silica gel chromatography). Unreacted tribromide **10** could easily be recovered during the purification of **12** (42.5% based on **10** used). Treatment of **12** with 1-octene in refluxing DME generated a free phosphine,[12] which underwent simultaneous intramolecular P-alkylation to give bicyclic phosphonium salt **13**. The phosphonium salt (**13**) was formed as a precipitate in the reaction mixture. After removal of soluble materials, crude

Scheme 1. Synthesis of Ph-SMAP (1a)

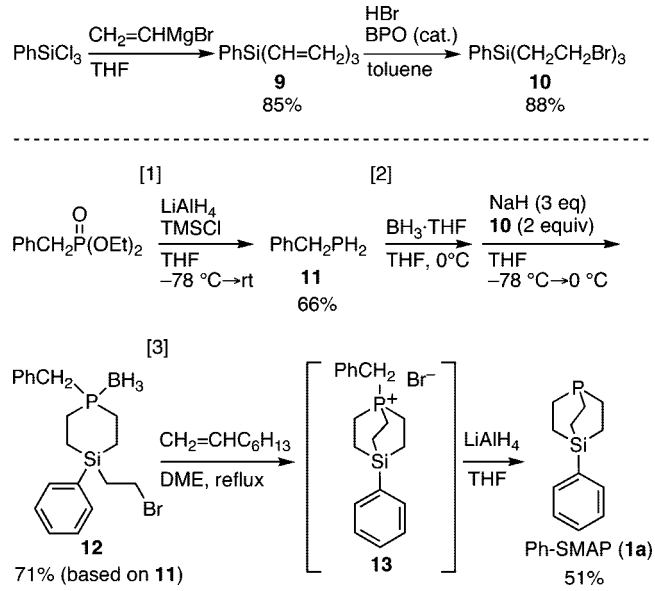

13 was used without further purification for the following one-pot reaction with $LiAlH_4$ that completed the synthesis of Ph-SMAP (51% after sublimation). Thus, Ph-SMAP was synthesized in three steps from diethyl benzylphosphonate with 24% overall yield.

Properties. Ph-SMAP is colorless crystalline solid with a sharp melting point of 90.5−90.7 °C (in a sealed tube). Purification of Ph-SMAP is easily performed upon sublimation (40 °C/0.04 mmHg). Being odorless, Ph-SMAP does not produce the noxious phosphine odor characteristic of volatile phosphines.

Solid Ph-SMAP is highly air-stable, with no detectable oxidation observed after exposure to air for several days. To our surprise, such stability was also observed in solution. A solution of Ph-SMAP in C_6D_6 prepared without exclusion of air underwent no oxidation detectable by ^1H NMR after standing for 3 days. Similar experiments with CD_2Cl_2 and acetone-d_6 produced only a trace amount (<3%) of the corresponding phosphine oxide after 1 h. This air stability is quite unusual as a property of a trialkylphosphine. Although the reason for the air stability is unclear, we speculate that it might arise from the geometrical constraint around the P atom, which limits the geometrical change that occurs in the pathway toward a transition state for the oxidation.

NMR Spectra. In the ^1H NMR spectrum of Ph-SMAP, the resonances of the methylene protons on the bicyclo[2.2.2]octane framework appeared as P-coupled multiplets with reasonable chemical shift values, displaying an AA′MM′ pattern (Figure 1a). It indicates that the geminal protons are chemically equivalent to each othersboth at α and β positions of the P atom.

In the $^{13}C\{^1H\}$ NMR spectrum, the signal for the *ipso*-carbon of the Si−phenyl group was observed as a doublet with a $^4J_{C-P}$ coupling constant of 4.5 Hz (Figure 1b). The long-range $^4J_{C-P}$ couplings were also observed for other bicyclic compounds **13**−**15** (Chart 3).[13] In contrast, no $^4J_{C-P}$ coupling was observed for monocyclic compound **12**. Thus, the long-range electronic

(10) Rosenberg, S. D.; Walburn, J. J.; Stankovich, T. D.; Balint, A. E.; Ramsden, H. E. *J. Org. Chem.* **1957**, *22*, 1200–1202.
(11) Horner, L.; Hoffmann, H.; Beck, P. *Chem. Ber.* **1958**, *91*, 1583–1588.
(12) Uziel, J.; Riege, N.; Aka, B.; Figuière, P.; Jugé, S. *Tetrahedron Lett.* **1997**, *38*, 3405–3408.

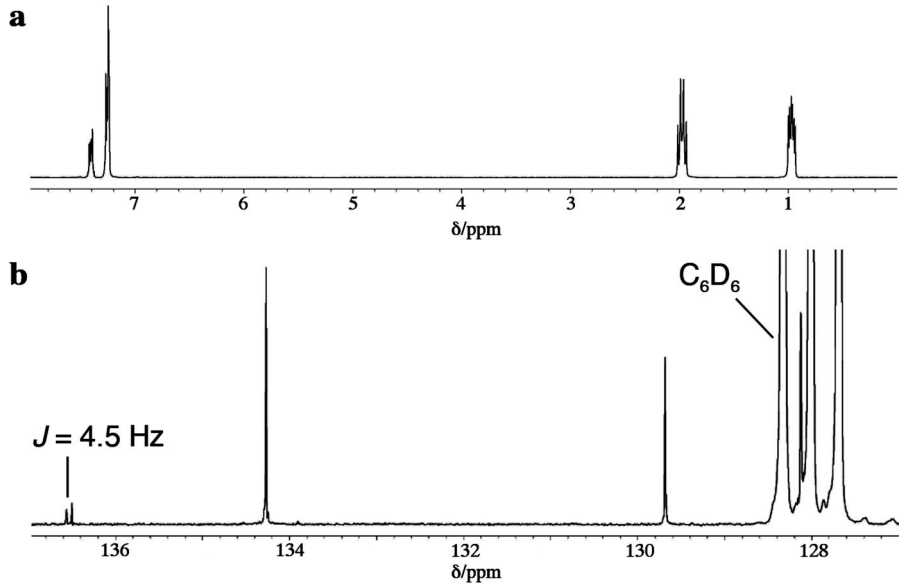

Figure 1. ^{1}H (a) and $^{13}C\{^{1}H\}$ (aromatic region) (b) NMR spectra of **1a**.

Chart 3. Long-Range C−P Coupling in the Cyclic Phosphorus Compounds

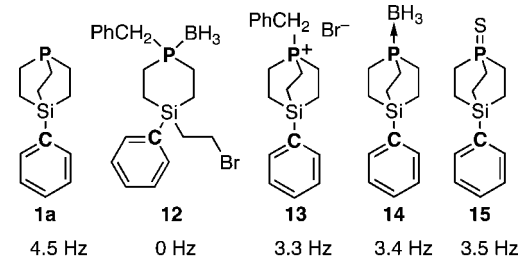

interaction is characteristic for the cage system, suggesting specific orbital interaction within the cage.[14]

X-ray Crystal Structures. Single-crystal X-ray diffraction analysis revealed a rodlike shape of Ph-SMAP **1a** and Ph-SMAP-BH_3 **14**[13] (Figure 2). Analysis also showed that the bicyclic cage possesses some flexibility and twists toward chiral C_3-symmetric conformations. In free phosphine **1a**, the values

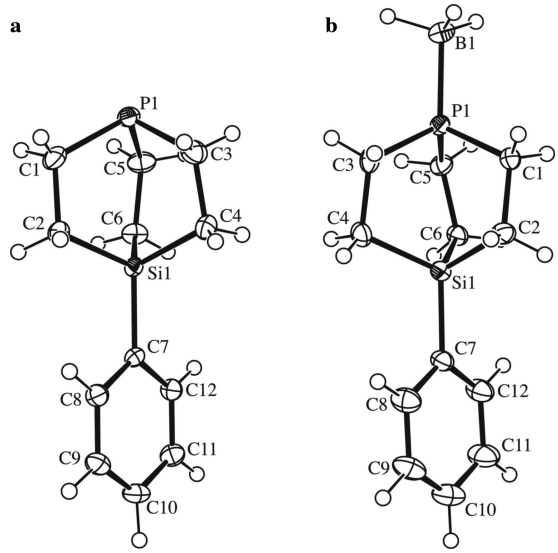

Figure 2. ORTEP drawings (50% probability level) for molecular structure of **1a** (a) and **14** (b).

Table 1. Selected Angles (deg) and P···Si Distances (Å) of 1a and 14

Ph-SMAP (**1a**)		Ph-SMAP-BH_3 (**14**)	
	Angles		
C(1)−P(1)−C(3)	100.42(8)	C(1)−P(1)−C(3)	103.4(1)
C(1)−P(1)−C(5)	101.17(8)	C(1)−P(1)−C(5)	103.9(1)
C(3)−P(1)−C(5)	101.12(8)	C(3)−P(1)−C(5)	105.2(1)
C(2)−Si(1)−C(4)	105.96(7)	C(2)−Si(1)−C(4)	104.3(1)
C(2)−Si(1)−C(6)	106.01(8)	C(2)−Si(1)−C(6)	104.4(1)
C(4)−Si(1)−C(6)	104.40(8)	C(4)−Si(1)−C(6)	105.2(1)
P(1)−C(1)−C(2)−Si(1)	−15.3(2)	P(1)−C(1)−C(2)−Si(1)	21.9(2)
P(1)−C(3)−C(4)−Si(1)	−17.3(2)	P(1)−C(3)−C(4)−Si(1)	23.6(2)
P(1)−C(5)−C(6)−Si(1)	−17.3(2)	P(1)−C(3)−C(4)−Si(1)	23.6(2)
	Distance (Å)		
P(1)···Si(1)	3.105	P(1)···Si(1)	3.031

for the average C−P−C and P−C−C−Si dihedral angles and the P−Si distance are 100.9°, 15.5°, and 3.105 Å, respectively. In BH_3 complex **14**, the P atom bonds to the B atom with a distance of 1.922(2) Å.[15] The average C−P−C angle is enlarged to 104.2° (Table 1). Such a slight enlargement of the angles around the P atom is typical for the metal coordination of a P-donor ligand. The BH_3 coordination also causes shrinkage of the cage as indicated by enlargement of the P−C−C−Si dihedral angles (22.3°, averaged) and shortening of the P−Si distance (3.031 Å). Although the cage possesses some flexibility for twisting and stretching, almost no bending of the longest molecular axes was observed for both **1a** and **14**.

Figure 3 represents the densely packed crystal structure of **1a** and **14**. The former consists of the two enantiomeric molecules ($P2_1/n$), while only a single enantiomer is involved in the latter (chiral space group $P2_1$). The latter is the case of chiral crystallization of an achiral molecule with a chiral conformation. The feature common to the crystal packing of **1a** and **14** is the columnar stacking along the *a*-axis through van der Waals contacts between neighboring 1-phospha-4-silabicyclo[2.2.2]octane cages. In both cases, the one-dimensional columns are further stacked along the longest molecular axis in a head-to-tail manner to form a sheet structure on the

(13) For isolation of **14** and **15**, see Supporting Information of ref 1a.

(14) The corresponding $^{4}J_{C\text{-}P}$ has not been observed in 9-phospha-10-silatriptycenes [**5** (R = Me, $C_{12}H_{25}$) and other derivatives]. See ref 5e.

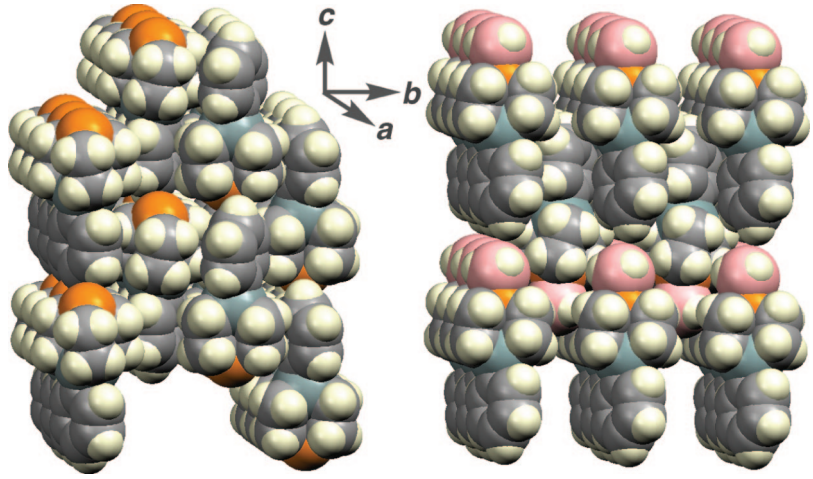

Figure 3. Crystal packing of Ph-SMAP (**1a**) and its BH_3 complex (**14**).

Table 2. Results of DFT Calculations for Various Tertiary Phosphines

entry	phosphine	V_{min} (kcal·mol^{-1})	av C−P−C angle (deg)[a]
1[b]	$(t\text{-Bu})_3P$	−45.48	107.5
2[b]	$(i\text{-Pr})_3P$	−44.47	101.6
3[b]	Et_3P	−43.51	99.5
4	Ph-SMAP (**1a**)	−43.14	99.7
5[b]	Me_3P	−43.02	99.4
6[b]	Me_2PhP	−40.41	
6[b]	**16**	−39.06	96.2
8[b]	$MePh_2P$	−36.76	

[a] Values of optimized structures. [b] Data are taken from ref 16.

a,*c* plane. In the case of **1a**, the sheets are then stacked along the *b*-axis so that the cage and the aromatic rings are alternatively arranged to allow van der Waals contacts. In contrast, the sheet of **14** is stacked through C−H···π interactions between neighboring aromatic rings.

Electronic Properties. DFT calculations [B3LYP/6-31G(d,p)] indicated that Ph-SMAP possesses an electron-donating ability as strong as that of Me_3P and that replacement of the Si atom of Ph-SMAP with a carbon atom drastically decreases the donor power. We optimized the geometry of Ph-SMAP and evaluated donor ability by the value of the molecular electrostatic potential minimum V_{min} (kcal·mol^{-1}) according to Koga's method.[16] A larger negative V_{min} value corresponds to a stronger electron-donating ability of a phosphine. For comparison, the calculations were carried out for 4-phenyl-1-phosphabicyclo[2.2.2]octane (**16**), an analogue of Ph-SMAP that has a bridgehead carbon atom instead of the Si atom.[17] As shown in Table 2, the V_{min} (−43.14 kcal/mol) of Ph-SMAP is much more negative than the value of monoaryldialkylphosphine $PhMe_2P$ and is in the range for trialkylphosphines, being between the values of Me_3P and Et_3P.

The V_{min} of **16** is less negative than that of $PhMe_2P$. The drastic decrease in donor ability upon placement of a carbon atom at the bridgehead is mostly due to the increase in s-character of the P lone pair caused by the strain in the 1-phosphabicyclo[2.2.2]octane cage. The strain is evident from the comparison of the C−P−C angles of the optimized structures (Figure 4); the average angle of **16** (96.2°) is much smaller than that of Ph-SMAP (99.7°), and the latter is almost the same as the values of Me_3P (99.4°) and Et_3P (99.5°).

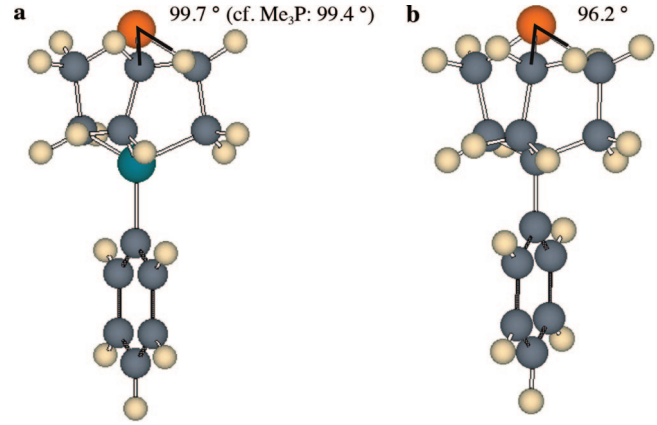

Figure 4. Optimized structures for Ph-SMAP (**1a**) (a) and for the carbon analogue (**16**) (b).

Transition Metal Complexes. A Vaska-type rhodium complex of Ph-SMAP, *trans*-[RhCl(CO)(Ph-SMAP)$_2$] (**17**) was obtained by the reaction of Ph-SMAP and [{RhCl(CO)$_2$}$_2$] (P/Rh = 2.1:1) in benzene at room temperature. The $^{31}P\{^1H\}$ NMR spectrum of **17** showed a doublet signal with a $^1J_{P-Rh}$ coupling of 117.8 Hz at δ −8.8 ppm. The infrared spectrum measured in a $CHCl_3$ solution gave a C−O stretching band at ν = 1965 cm^{-1}. This C−O stretching is 2 cm^{-1} lower in wavenumber than the value for the corresponding Me_3P complex,[18] which was obtained by the measurement under the identical conditions. The shift of wavenumber may be due to the increased donor power of Ph-SMAP (**1a**) as compared with that of Me_3P.

The molecular structure of **17** was determined by single-crystal X-ray diffraction. An ORTEP diagram is shown in Figure 5, and selected bond distances and angles are listed in Table 3. The structure was solved as being C_2 symmetric for an axis going through the Rh atom bearing the disordered Cl and CO ligands. Owing to the trans geometry of Ph-SMAP with rigid

(15) (a) The P−B bond length of **14** (1.922(2) Å) is apparently longer than that of Me_3P-BH_3 (1.901 Å) determined by microwave spectroscopy. See: Bryan, P. S.; Kuczkowski, R. L. *Inorg. Chem.* **1972**, *11*, 553–559. (b) The reason of the elongation is not clear at present. Correlation between steric/electronic properties of phosphines and P−B bond lengths are not clear in general. For a review, see: Brunel, J. M.; Faure, B.; Maffei, M. *Coord. Chem. Rev.* **1998**, *178*−*180*, 665–698.

(16) Suresh, C. H.; Koga, N. *Inorg. Chem.* **2002**, *41*, 1573–1578.

(17) The phosphine oxide form of 1-phosphabicyclo[2.2.2]octane was synthesized and its strain around the P atom was discussed. But it has not been converted to the free phosphine. See: Wetzel, R. B.; Kenyon, G. L *J. Am. Chem. Soc.* **1974**, *96*, 5189–5198.

(18) Boyd, S. E.; Field, L. D.; Hambley, T. W.; Partridge, M. G. *Organomatallics* **1993**, *12*, 1720–1724.

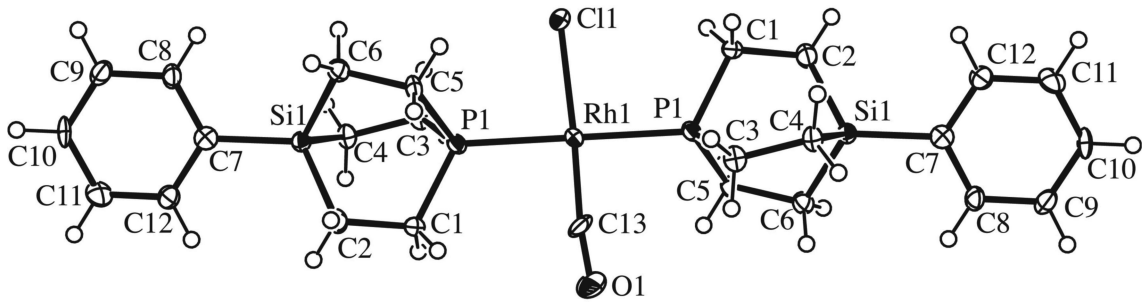

Figure 5. ORTEP drawing (50% probability level) with atom-labeling scheme for the molecular structure of *trans*-[RhCl(CO)(Ph-SMAP)$_2$] (**17**).

Table 3. Selected Bond Lengths (Å) and Angles (deg) of 17

	Lengths		
Rh(1)−Cl(1)	2.364(4)	Rh(1)−C(13)	1.75(2)
Rh(1)−P(1)	2.316(1)	C(13)−O(1)	1.18(2)
	Angles		
Cl(1)−Rh(1)−P(1)	93.67(9)	C(2)−Si(1)−C(4)	103.8(2)
C(13)−Rh(1)−P(1)	89.0(5)	C(2)−Si(1)−C(6)	103.6(2)
C(1)−P(1)−C(3)	102.0(2)	C(4)−Si(1)−C(6)	104.8(2)
C(1)−P(1)−C(5)	102.3(2)	P(1)−C(1)−C(2)-Si(1)	29.1(4)
C(3)−P(1)−C(5)	103.8(2)	P(1)−C(3)−C(4)-Si(1)	28.1(4)
C(13)−Rh(1)−P(1)	89.0(5)	C(2)−Si(1)−C(6)	103.6(2)

and linear structure features, the entire molecule displays a rodlike structure. The C−O bond length [1.18(2) Å] of the carbonyl ligand is significantly longer than the reported value [1.146(4) Å] for the Me_3P complex.[18] This observation is consistent with the results of the IR measurements and the DFT calculations.

An organoplatinum(II) complex with cis-coordinated Ph-SMAP ligands, *cis*-[$PtMe_2$(Ph-SMAP)$_2$] (**18**) was obtained by the reaction of Ph-SMAP and *cis*-[$PtMe_2(\eta^2,\eta^2$-1,5-cyclooctadiene)] (P/Pt; 2.2:1) in benzene-d_6 at room temperature. The $^{31}P\{^1H\}$ NMR spectrum showed a singlet signal at δ −21.3 accompanied by a ^{195}Pt satellite with J_{P-Pt} value of 1785 Hz.

Single crystals of platinum complex **18** with a composition of $PtMe_2$(Ph-SMAP)$_2\cdot$(hexane)$_{0.5}$ were obtained by recrystallization from CH_2Cl_2/hexane. An ORTEP diagram of the molecular structure determined by X-ray diffraction is shown in Figure 6. Selected bond lengths and angles are listed in Table 4. The two Ph-SMAP ligands on the Pt atom adopt considerably different conformations to each other with respect to the extent of twisting in the bicyclic system. While one adopts a normal twisted conformation, the bicyclic system of the other is rather eclipsed.

Owing to the cis geometry of the rod-shaped Ph-SMAP ligands, the platinum complex displays an L-shaped molecular structure with the platinum atom at the corner. The crystal-packing diagrams (Figure 7) show a supramolecular structure with square channels filled with hexane molecules. Continuous head-to-tail intermolecular C−H$\cdots\pi$ interactions between the aromatic rings form a columnar stack of angular figures of eight along the *a* axis creating a pair of square channels, which accommodate a train of the hexane molecules with a fully extended conformation. Although the C−H$\cdots\pi$ molecular interaction is too weak for **18** to be used as functional materials such as metal−organic framework (MOF), the novel molecular arrangement of **18** implies that SMAP derivatives with an appropriate functional group that allows for more strong molecular interactions may be useful as an element of molecular architecture toward functional materials.

Applications to Transition Metal Catalysis. Our experiments in the applications of Ph-SMAP (**1a**) to the rhodium-catalyzed hydrosilylation and hydrogenation of ketones revealed unique properties and usefulness of Ph-SMAP as a ligand for transition metal catalysis.

1. Rh-Catalyzed Hydrosilylation of Ketones with Triorganosilanes. The hydrosilylation of cyclohexanone (**19**) (1 mmol) with $PhMe_2SiH$ (1.2 mmol) was carried out in benzene (1 mL) at room temperature (25 °C) in the presence of [{RhCl(C_2H_4)$_2$}$_2$] (0.5 mol %) and a phosphine ligand (1 mol %, Rh/P 1:1) (Scheme 2). Time−conversion curves for the reactions with Ph-SMAP (**1a**) and other conventional phosphines including Me_3P, Et_3P, Bu_3P, (*c*-Hex)$_3P$, (*t*-Bu)$_3P$, and Ph_3P are given in Figure 8a. Ph-SMAP (**1a**) was distinguished with its high rate-enhancement effect among the ligands tested: completion was reached within 1 h. A very interesting observation is that Me_3P (1 M toluene solution was used) was much less efficient in the rate enhancement than **1a**, while having comparable compactness and electron-donating ability. The lower efficiency of the Me_3P might be attributable to lability of the C−H bonds of the Me groups toward intramolecular C−H bond actvation, albeit with no experimental proof. On the other hand, Ph-SMAP is expected to be inert toward α C−H bond activation because of the molecular constraint.

The catalytic activity of [{RhCl(C_2H_4)$_2$}$_2$]/Ph-SMAP (Rh/P 1:1) system is comparable or even higher than those of the recently reported, highly active, homogeneous Rh catalysts that involve bulky, monocoordinating ligands such as the bowl-shaped phosphine (BSP, **20**),[19] the triethynylphosphine with bulky end caps (**21**),[20] and the bulky terphenylisocyanide (**22**) (Chart 4):[21] the reactions with [{RhCl(C_2H_4)$_2$}$_2$]/**20** (Rh/P 1:2), [{RhCl(cod)}$_2$]/**21** (Rh/P 1:1) and [Rh(cod)$_2$]BF_4/**22** (Rh/isocyanide 1:1) required 3, 2 and 1 h for completion, respectively, under otherwise same conditions.

When **1a** was used with Rh/P ratio of 1:2, rapid reaction was initiated after a 2 h induction period, completing within 5 h (Figure 8b). An active species must have been formed through the dissociation or reaction of the ethylene ligands accompanied by metal−ligand dissproportionation. The fact that the reaction was faster with Rh/P ratio of 1:1 than with 1:2 suggests that

(19) (a) Niyomura, O.; Tokunaga, M.; Obora, Y.; Iwasawa, T.; Tsuji, Y. *Angew Chem., Int. Ed.* **2003**, *42*, 1287–1289. (b) Niyomura, O.; Iwasawa, T.; Sawada, N.; Tokunaga, M.; Obora, Y.; Tsuji, Y. *Organometallics* **2005**, *24*, 3468–3475.

(20) Ochida, A.; Sawamura, M. *Chem. Asian J.* **2007**, *2*, 609–618.

(21) (a) Ito, H.; Kato, T.; Sawamura, M. *Chem. Lett.* **2006**, *35*, 1038–1039. (b) Ito, H.; Kato, T.; Sawamura, M. *Chem. Asian J.* **2007**, *2*, 1436–1446.

(22) The Rh−**1a** system showed no activity for the hydrosilylation of dipropyl ketone (**26**) with $PhSiH_3$ and $(EtO)_3SiH$ under the otherwise the same reaction conditions, while Ph_2SiH_2 was more reactive than $PhMe_2SiH$. The reaction led to >95% conversion after 10 min with both Ph-SMAP (**1a**) and Ph_3P as determined by GC analysis of 4-heptanol (isolation of the silyl ether product has not been attempted).

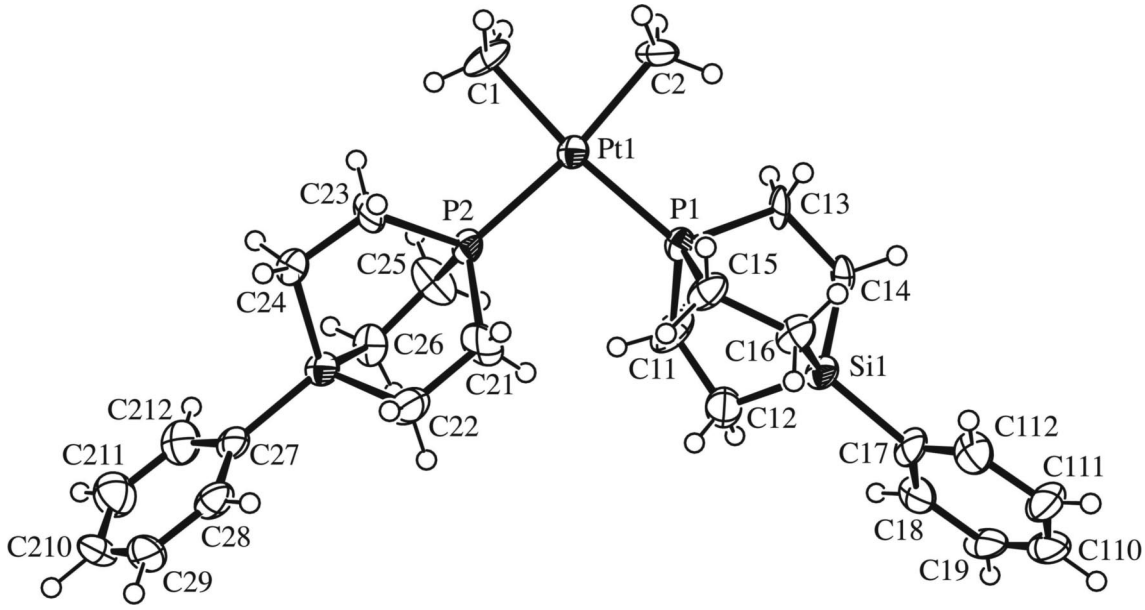

Figure 6. ORTEP drawing (50% probability level) with atom-labeling scheme for the molecular structure of *cis*-[$PtMe_2$(Ph-SMAP)$_2$] (**18**).

Table 4. Selected Bond Lengths (Å), Angles (deg), and Dihedral Angles (deg) of 18

	Bond Lengths		
Pt(1)−P(1)	2.286(3)	Pt(2)−P(2)	2.293(3)
Pt(1)−C(1)	2.10(1)	Pt(2)−C(2)	2.293(3)
	Angles		
P(1)−Pt(1)−P(2)	97.4(1)	C(21)−P(2)−C(25)	102.2(8)
P(1)−Pt(1)−C(2)	90.1(4)	C(23)−P(2)−C(25)	101.7(7)
P(2)−Pt(1)−C(1)	89.2(5)	C(12)−Si(1)−C(14)	103.3(7)
C(1)−Pt(1)−C(2)	83.9(6)	C(12)−Si(1)−C(16)	106.2(6)
C(11)−P(1)−C(13)	97.5(7)	C(14)−Si(1)−C(16)	102.2(6)
C(11)−P(1)−C(15)	103.9(8)	C(22)−Si(2)−C(24)	104.0(7)
C(13)−P(1)−C(15)	101.2(6)	C(22)−Si(2)−C(26)	106.2(6)
C(21)−P(2)−C(23)	99.9(8)	C(24)−Si(2)−C(26)	105.2(6)
	Dihedral Angles		
P(1)−C(11)−C(12)−Si(1)	−33(1)	P(2)−C(21)−C(22)−Si(2)	9(1)
P(1)−C(13)−C(14)−Si(1)	−25(1)	P(2)−C(23)−C(24)−Si(2)	10(1)
P(1)−C(15)−C(16)−Si(1)	−29(1)	P(2)−C(25)−C(26)−Si(2)	8(1)

the active species is a Rh−**1a** 1:1 complex. This assumption is consistent with the previous results with the bulky ligands such as **20**−**22**[19−21] as well as the solid-supported SMAP derivative Silica-SMAP (**7**),[8] while the catalyst with the latter exhibited exceptionally high catalytic activity (<5 min for 100% conversion).

Next, we examined some other ketones (**23**−**27**) with different steric and electronic properties for reactivity toward the hydrosilylation wth $PhMe_2SiH$ catalyzed by the Rh-**1a** system (Rh/P 1:1) under the conditions optimized for cyclohexanone (**19**). Results are summarized in Chart 5. The reactions of 2-methylcyclohexanone (**23**) and diethyl ketone (**24**) proceeded smoothly and completed within 2 and 5 h, respectively, while the reactions of acetophenone (**25**) and di-*n*-propyl ketone (**26**) were somewhat slower (**25**, 5 h, 93% conversion; **26**, 8 h, 83% conversion). Although the Rh-**1a** catalyst showed activity toward sterically more demanding, diisopropyl ketone (**27**), the reaction was sluggish at 25 °C (72 h, 72% conversion). In sharp contrast to the activity of the Silica-SMAP-Rh catalyst, the Rh-**1a** catalyst showed very low activity toward the reaction with Et_3SiH (**19**, 5 h, 8% conversion; **27**, 24 h, 0% conversion). No reaction was observed for the hydrosilylation of cyclohexanone (**19**) with (*t*-Bu)Me_2SiH.

2. Rh-Catalyzed Hydrogenation of Ketones. Hydrogenation of ketones is feasible with various types of catalysts under

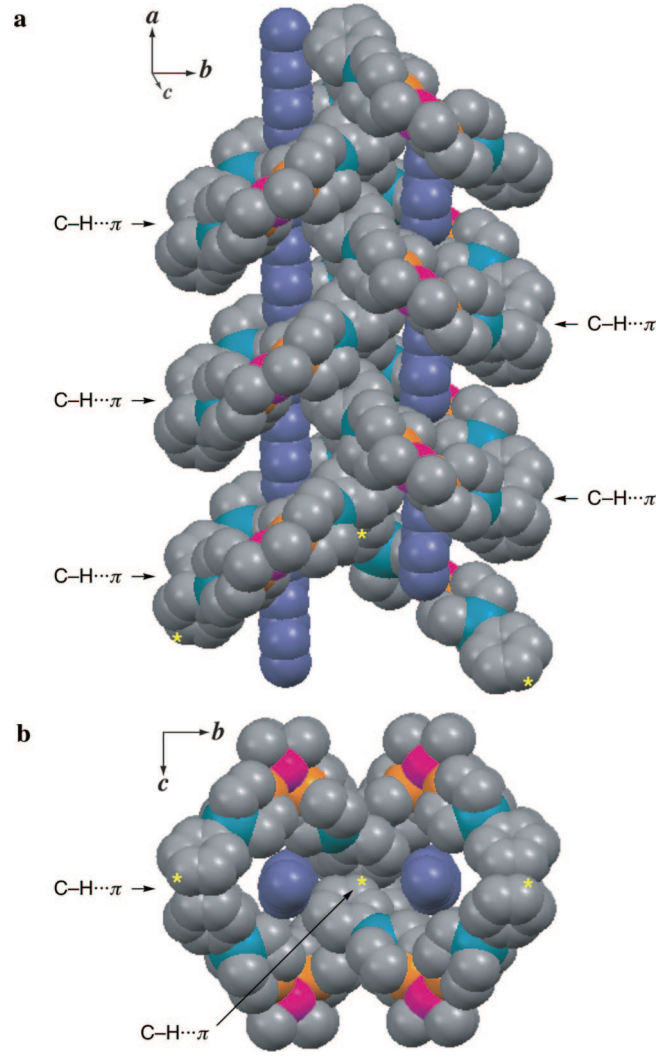

Figure 7. Crystal-packing diagrams of *cis*-[$PtMe_2$(Ph-SMAP)$_2$]·(hexane)$_{0.5}$ with a view along the *c* axis (side view) (a) and with a view along the *a* axis (bottom view) (b).

Chart 4. Bulky Ligands Used for the Rh-Catalyzed Hydrosilylation of Ketones

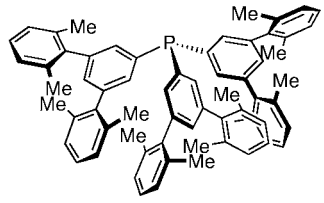

20
Bowl-shaped phosphine

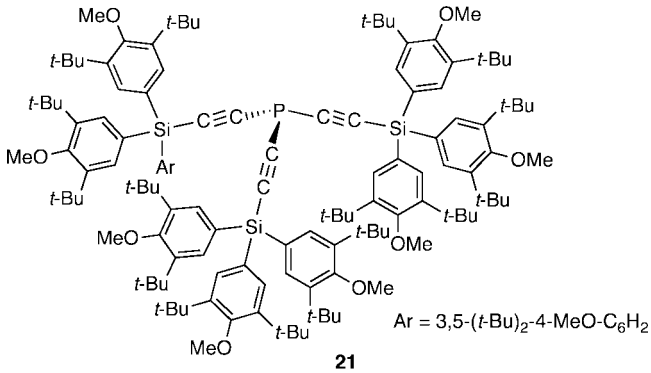

21
Triethynylphosphine with bulky end caps

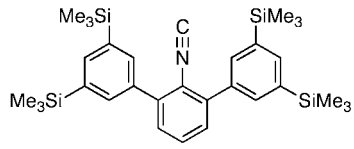

22
Bulky isocyanide

Scheme 2. Rh-Catalyzed Hydrosilylation of Cyclohexanone (19) with $PhMe_2SiH$

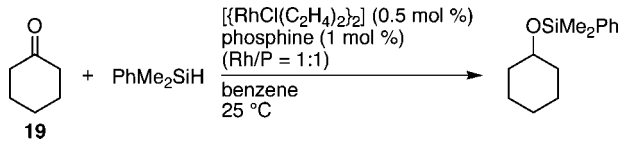

19

transfer hydrogenation conditions that employ secondary alcohols as a hydrogen source,[23] but catalysts effective for the hydrogenation of simple, nonchelating ketones with molecular hydrogen are not so common.[24] In particular, the hydrogenation of hindered ketones is extremely difficult.[25]

The Ph-SMAP ligand showed high performance for the Rh-catalyzed hydrogenation of ketones with molecular hydrogen, especially toward the reaction of hindered ketones. Thus, the hydrogenation of diisopropyl ketone (**27**) proceeded in the presence of a rhodium catalyst prepared in situ from [{Rh(OMe)-(cod)}$_2$] (0.5 mol %) and Ph-SMAP (**1a**) (1 mol %, Rh/P 1:1)with 30 atm of initial hydrogen pressure at 100 °C in THF, showing 46% conversion to the corresponding alcohol after 20 h (48%, 48 h) (Table 5, entry 1). Owing to the steric congestion of the carbonyl group, diisopropyl ketone (**27**) is an extremely challenging substrate for catalytic hydrogenation.[25] In fact, the hydrogenation of **27** showed only a trace of conversion when Me_3P and Bu_3P were employed as a ligand (Rh/P 1:1) under otherwise identical conditions, and did not take place at all with $(t\text{-Bu})_3P$, PPh_3 (Rh/P 1:1) and dppe (Rh/P 1:2) (Table 5, entries 4−8). The inferiority of Me_3P as compared with Ph-SMAP is to be noted: it may, in part, be due to its high volatility at the high reaction temperature or to lability of the C−H bonds of the P-Me groups as in the case of the hydrosilylation (vide info).

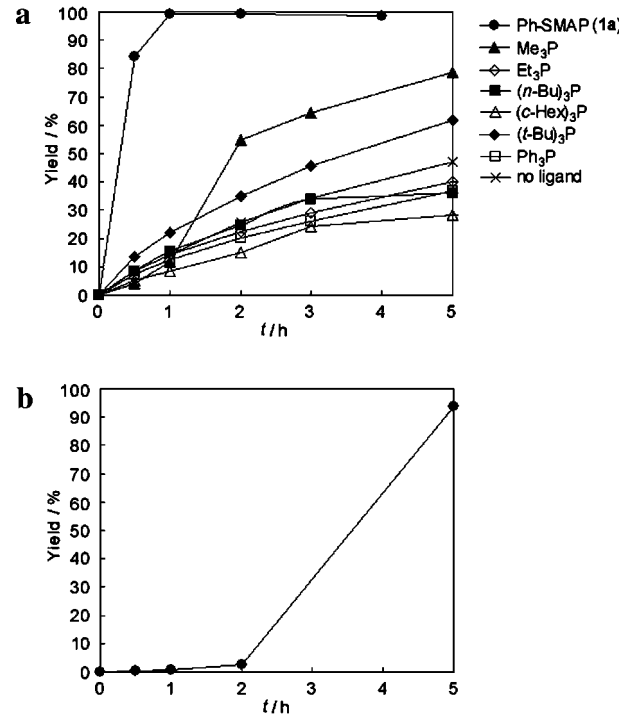

Figure 8. Time−conversion curves for the Rh-catalyzed hydrosilylation of cyclohexanone (**19**) (1 mmol) with $PhMe_2SiH$ (1.2 mmol) in benzene (1 mL) at 25 °C. Yields were obtained by GC. (a) The catalysts were prepared in situ from [{RhCl$(C_2H_4)_2$}$_2$] (0.5 mol %) and the phosphine (1 mol %, Rh/P 1:1). Results in the absence of a phosphine ligand are also shown. (b) The catalyst was prepared in situ from [{RhCl$(C_2H_4)_2$}$_2$] (0.5 mol %) and **1a** (2 mol %, Rh/P 1:2).

Chart 5. Results (Reaction Time and Conversion) of Hydrosilylation of Various Ketones with $PhMe_2SiH$ Catalyzed by the Rh−1a System (Rh/P1:1)[a]

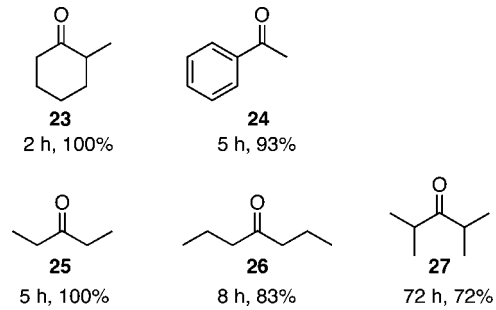

23 2 h, 100% **24** 5 h, 93%

25 5 h, 100% **26** 8 h, 83% **27** 72 h, 72%

[a] Conditions: ketone (1 mmol), $PhMe_2SiH$ (1.2 mmol), [{RhCl-$(C_2H_4)_2$}$_2$] (0.5 mol %), **1a** (1 mol %; Rh/P 1:1), benzene (1 mL), 25 °C.

(23) Klomp, D.; Hanefeld, U.; Peters, J. A. In *Handbook of Homogeneous Hydrogenation*; de Vries, J. G., Elsevier, C. J., Eds.; Wiley-VCH: Weinheim, Germany, 2007; Vol. 2, pp 585−630.

(24) Blum, Y.; Czarkle, D.; Rahamim, Y.; Shvo, Y. *Organometallics* **1985**, *4*, 1459–1461.

(25) (a) Diisopropyl ketone (**27**) could not be reduced with Raney nickel or with nickel and some promoters, but was finally reduced with an equal weight of catalyst promoted with chloroplatinic acid and sodium hydroxide. See: Blance, R. B.; Gibson, D. T. *J. Chem. Soc.* **1954**, 2487–2489. (b) See also: Freiferder, M. In *Catalytic Hydrogenation in Organic Synthesis. Procedures and Commentary*; Wiley: New York, 1978; Chapter 9, pp 78−89.

Table 5. Ligand Effect in the Rh-Catalyzed Hydrogenation of Various Ketones[a]

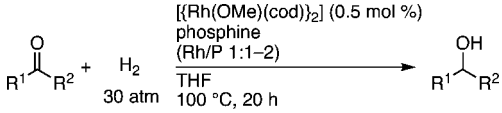

entry	ketone	phosphine	Rh/P	conv., %[b]
1	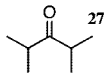 **27**	Ph-SMAP (**1a**)	1:1	46 (48)[c]
2		Ph-SMAP (**1a**)	1:2	0
3		none	N.A.	0
4		Me_3P	1:1	1
5		Bu_3P	1:1	4
6		$(t\text{-}Bu)_3P$	1:1	0
7		Ph_3P	1:1	0
8		$Ph_2PCH_2CH_2PPh_2$	1:2	0
9	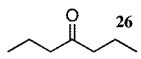 **26**	Ph-SMAP (**1a**)	1:1	70
10		Me_3P	1:1	trace
11	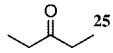 **25**	Ph-SMAP (**1a**)	1:1	97
12		Me_3P	1:1	3
13	 **19**	Ph-SMAP (**1a**)	1:1	100
14		Me_3P	1:1	54

[a] Conditions: ketone (1 mmol), H_2 (30 atm), [{Rh(OMe)(cod)}$_2$] (0.005 mmol), phosphine (0.01−0.02 mmol), THF (1 mL), 100 °C, 20 h. [b] Conversion of ketone into alcohol determined by GC. [c] Value in parentheses is conversion after 48 h.

Neither phosphine-free [{Rh(OMe)(cod)}$_2$] (Table 5, entry 3) nor Wilkinson's catalyst ([$RhCl(PPh_3)_3$]) were capable of promoting the reaction.

The second equivalent of Ph-SMAP (**1a**) (Rh/P 1:2) completely inhibited the activity of the Rh-Ph-SMAP catalyst in the hydrogenation of **27** (Table 5, entry 2). This result suggests that an active catalytic species might carry only one Ph-SMAP ligand. According to this assumption, the fact that the reaction catalyzed by the Rh-Ph-SMAP (Rh/P 1:1) system almost ceased to proceed at 20 h can be explained by considering the metal−ligand disproportionation that formed inactive rhodium species with more than two Ph-SMAP ligands and phosphine-free rhodium species.

The superiority of Ph-SMAP over Me_3P was not limited to the hydrogenation of the bulky ketone (**27**), but was also observed for the case of less hindered, more reactive ketones such as dipropyl ketone (**26**), diethyl ketone (**25**), and cyclohexanone (**19**). These ketones were hydrogenated with the Rh-Ph-SMAP system with 70%, 97%, and 100% conversions, respectively, under the conditions (Rh/P 1:1, H_2 30 atm, THF, 100 °C, 20 h) that promoted the hydrogentaion of diisopropyl ketone (**27**) with 46% conversion (Table 5, entries 9, 11, and 13), while the hydrogenation with Me_3P resulted in <1% (trace), 3% and 54% conversions, respectively (Table 5, entries 10, 12, and 14).

Conclusions

A caged trialkylphosphine with extremely small steric demand and strong electron-donating ability, 4-phenyl-1-phospha-4-silabicyclo[2.2.2]octane (Ph-SMAP), was synthesized. Although the new phosphine is comparable to Me_3P in both steric demand and electronic property, it is air stable even in solution, nonvolatile, and easy to handle. Furthermore, Ph-SMAP displayed high performance as a ligand for the Rh-catalyzed hydrosilylation and hydrogenation of simple, nonchelating ketones, especially for the reaction of hindered ketones. Therefore, Ph-SMAP is not an analogue of Me_3P but a new type of phosphine ligand useful for studies in organic and inorganic chemistry as well as transition metal catalysis.

Experimental Section

General. NMR spectra were recorded on a Varian Gemini 2000 spectrometer, operating at 300 MHz for ^1H NMR, 75.4 MHz for $^{13}C\{^1H\}$ NMR, and 121.4 MHz for $^{31}P\{^1H\}$ NMR. Chemical shift values for ^1H, $^{13}C\{^1H\}$, and $^{31}P\{^1H\}$ NMR are reference to Me_4Si, the residual solvent resonances, and external aqueous 85% H_3PO_4 respectively. Chemical shifts are reported in δ ppm. Mass spectra were obtained by APCI method with a JEOL JMS-T100LC. Infrared spectra were recorded on Perkin-Elmer Spectrum One. Only characteristic peaks are reported in cm^{-1}. Elemental analysis was performed at the Center for Instrument Analysis of Hokkaido University. DFT calculations [B3LYP/6-31G(d,p)] were performed with the Gaussian 98 program at the Hokkaido University Information Initiative Center. Anhydrous solvents were purchased from Kanto Chemical Co. and used without further purification. [{Rh(OMe)(cod)}$_2$] was purchased from Sigma-Aldrich Inc. [{$RhCl(CO)_2$}$_2$] was purchased from Wako Pure Chemical Industries, Ltd.

Phenyltrivinylsilane (9).[10] Under an argon atmosphere, gaseous vinyl bromide (201.3 g, 1.88 mol) was dissolved in THF (150 mL) at −78 °C. The solution was added dropwise to Mg (45.7 g, 1.88 mol) in THF (150 mL) at room temperature over 3 h. After stirring at room temperature for 1 h, a solution of trichlorophenylsilane (96 mL, 0.6 mol) in THF (400 mL) was added dropwise at room temperature over 3.5 h. After stirring at room temperature overnight, a total of 300 mL of saturated aq NH_4Cl was gradually added to the mixture at 0 °C to cause clear phase separation (clear yellow solution and white solid). The solid was filtrated on a pad of Celite and was washed with diethyl ether. The solution was dried over $MgSO_4$ and evaporated. Distillation (66−67 °C at 280 Pa) of the mixture gave **9** (94.3 g, 0.51 mol, 84%) as colorless oil.

Tris(2-bromoethyl)phenylsilane (10). Hydrogen bromide, which was generated by slowly adding bromine (2.52 mol, 129 mL) to 1,2,3,4-tetrahydronaphthalene (3.47 mol, 470 mL) at room temperature, was bubbled through a stirred solution of **9** (0.63 mol, 117.43 g) in toluene (1.6 L) at room temperature. After the reaction mixture was stirred overnight, saturated aq $NaHCO_3$ and aq $Na_2S_2O_3$ were added. The resultant mixture was extracted with diethyl ether three times. The extract was dried over $MgSO_4$ and filtered. The combined filtrate and washings were concentrated. Purification by recrystallization from ethanol gave **10** as a colorless solid (232.44 g, 86%). Mp: 66.8−67.5 °C. ^1H NMR (300 MHz, $CDCl_3$): δ 1.71−1.76 (m, 6H, $-SiCH_2CH_2Br$), 3.48−3.54 (m, 6H, $-SiCH_2CH_2Br$), 7.43−7.47 (m, 5H, Ar*H*). ^{13}C NMR (75.4 MHz, $CDCl_3$): δ 19.0 (s, $-SiCH_2CH_2Br$), 29.0 (br s, $-SiCH_2CH_2Br$), 128.7 (s, *C*H), 130.6 (s, *C*H), 131.5 (s, *C*), 133.8 (s, *C*H). Anal. Calcd for $C_{12}H_{17}Br_3Si$: C 33.59%, H 3.99%, Br 55.87%. Found: C 33.48%, H 3.93%, Br 56.00%.

Benzylphosphine (11).[11] Under an argon atmosphere, chlorotrimethylsilane (47.3 mL, 374 mmol) was added dropwise to a suspension of $LiAlH_4$ (13.7 g, 360 mmol) in THF (400 mL) at −78 °C over 20 min. After stirring at −78 °C for 3 h, $PhCH_2P(O)(OEt)_2$ (50 mL, 240 mmol, prepared from benzyl bromide and triethyl phosphite) was added dropwise at −78 °C over 3.5 h. After stirring at room temperature overnight, the mixture was cooled to 0 °C. Degassed water (13.7 mL), 15 wt % aq NaOH (13.7 mL), and water (41.1 mL) were successively added at 0 °C.

After stirring at room temperature for 1 h, the mixture was filtered and washed with THF. Distillation of the solution (73−74 °C at 8 hPa) gave **11** (19.61 g, 158 mmol, 66%) as colorless oil.

1-Boranato-4-(2-bromoethyl)-1-benzyl-4-phenyl-1-phospha-4-silacyclohexane (12). To a BH_3−THF solution (100 mL, 99 mmol, 0.99 M in THF) was added **11** (11.2 g, 90.2 mmol) at 0 °C. The mixture was stirred at 0 °C for 19 h. The solution was transferred over a period of 1 h through a Teflon cannula tube to a mixture of NaH (10.8 g, 270.6 mmol, 60% in oil) and **10** (77.4 g, 180.4 mmol) in degassed THF (180 mL), which was cooled at −78 °C. The mixture was allowed to warm to 4 °C with stirring over a period of 20 h. Saturated aq NH_4Cl (400 mL) was carefully added, and the mixture was extracted twice with ether. The combined extracts were dried over $MgSO_4$ and filtered. After concentration under reduced pressure, purification by flash chromatography on silica gel (silica gel; 400 g for making a column and 100 g for charging the mixture, CH_2Cl_2/hexane 5:95−50:50) gave unreacted tribromide **10** (32.89 g, 42.5% based on the amount used) and **12** as a colorless waxy solid (25.80 g, 71%, cis/trans mixture). ^{1}H NMR (300 MHz, $CDCl_3$): δ 1.12−1.93 (m, 10H), 2.95 (d, J = 11.2 Hz, 1H), 3.11 (d, J = 11.0, 1H), 3.38−3.45 (m, 2H), 7.07−7.47 (m, 10H). ^{13}C NMR (75.4 MHz, $CDCl_3$): δ 4.48 (s) and 4.82 (d, J_{C-P} = 1.7 Hz, 4C), 17.9 and 18.1 (d, J_{C-P} = 33.8 Hz, 4C), 18.8 and 20.7 (s, 2C), 29.8 and 29.9 (s, 2C), 31.8 and 32.8 (d, J_{C-P} = 30.3 Hz, 31.5 Hz, respectively, 2C), 127.1 and 127.3 (d, J_{C-P} = 2.9 Hz, 2C), 128.5 and 128.6 (s, 2C), 128.6 and 128.8 (d, J_{C-P} = 2.8 Hz, 2.2 Hz, respectively, 1C), 129.6 and 129.7 (d, J_{C-P} = 4.0 Hz, 2C), 130.3 and 130.4 (s, 2C), 132.0 and 132.1 (d, J_{C-P} = 6.9 Hz, 1C), 132.5 and 132.8 (s, 1C), 133.8 and 133.9 (s, 2C). ^{31}P NMR (121.4 MHz, $CDCl_3$): δ 13.0 (br s). HRMS (FAB): Calcd for $C_{19}H_{27}BPSiBrNa$ $[M + Na]^+$ (m/z): 427.0798. Found: 427.0810.

1-Benzyl-4-phenyl-1-phosphonia-4-silabicyclo[2.2.2]octane bromide (13) (an Intermediate in the Conversion of 12 to 1a). Although the protocol for the synthesis of Ph-SMAP (**1a**) does not involve the isolation of this compound, it could alternatively be isolated and characterized as follows. A solution of 1-octene (5.8 mL, 37 mmol) and **10** (1.5 g, 3.7 mmol) in DME (185 mL) was degassed by three freeze−pump−thaw cycles and refluxed for a week. The reaction mixture was cooled to room temperature. Solids in the mixture were filtered and washed with Et_2O/hexane (1:1). The powder was dried under a reduced pressure. Purification by flash chromatography on silica gel (MeOH/$CHCl_3$ 3:97) gave the title compound as colorless crystals (0.955 g, 66%). Mp 225.0−226.3 °C. ^{1}H NMR (300 MHz, $CDCl_3$): δ 1.39−1.49 (m, 6H), 2.96−3.06 (m, 6H) 4.40 (d, J = 16.8 Hz, 2H), 7.28−7.50 (m, 10H). ^{13}C NMR (75.4 MHz, $CDCl_3$) δ 3.19 (d, J_{C-P} = 4.6 Hz, 3C), 14.74 (d, J_{C-P} = 49.8 Hz, 3C), 27.7 (d, J_{C-P} = 41.8 Hz, 1C), 128.2 (d, J_{C-P} = 9.7 Hz, 1C), 128.4 (d, J_{C-P} = 3.4 Hz, 1C), 128.5 (s, 2C), 129.4 (d, J_{C-P} = 3.4 Hz, 2C), 129.9 (d, J_{C-P} = 3.3 Hz, 1C), 130.2 (d, J_{C-P} = 5.2 Hz), 131.1 (s, 1C), 133.8 (s, 2C). ^{31}P NMR (121.4 MHz, $CDCl_3$): δ 14.3 (s). HRMS (EI): Calcd for $C_{19}H_{23}PSi$ $[M-HBr]^+$ (m/z): 310.1307. Found: 310.1308.

4-Phenyl-1-phospha-4-silabicyclo[2.2.2]octane (Ph-SMAP, 1a).[1a] A solution of 1-octene (2.9 mL, 21.3 mmol) and **10** (1.08 g, 2.67 mmol) in DME (30 mL) was degassed by three freeze−pump−thaw cycles and refluxed for 5 days. The reaction mixture was cooled to room temperature. The liquid was removed with a cannula, and the remaining solid was washed with Et_2O/hexane (1:1, 10 mL × 3). THF (30 mL) was added, and the mixture was degassed as above. $LiAlH_4$ (203 mg, 5.34 mmol) was added, and the mixture was stirred at room temperature for 18 h. Degassed water (0.2 mL) was carefully added to the ice-cooled, well-stirred mixture. The mixture was then treated successively with 15% aq NaOH (0.2 mL) and with water (0.6 mL) at 0 °C. After stirring was continued for 30 min at room temperature, the mixture was filtered through a pad of Celite on a glass filter (open air) and the solid was washed with degassed ether. The filtrate was concentrated to leave 481 mg of white solid. The solid was treated with degassed benzene and the mixture, which contained a considerable amount of insoluble solid, was passed through a short-pass column of alumina. The mixture was concentrated in a sublimation apparatus. Purification by sublimation (60−80 °C, 20 Pa) gave 300.4 mg (50.8%) of **1a** as cubic crystals. Mp: 90.5−90.7 °C (in a sealed tube). ^{1}H NMR (300 MHz, C_6D_6): δ 0.84−0.90 (m, 6H), 1.84−1.91 (m, 6H), 7.16−7.17 (m, 3H), 7.29−7.33 (m, 2H).^{13}C NMR (75.4 MHz, C_6D_6): δ 4.35 (3C), 18.0 (d, J_{C-P} = 16.0 Hz, 3C), 128.1 (2C), 129.7 (1C), 134.3 (2C), 136.5 (d, J_{C-P} = 4.5 Hz, 1C). ^{31}P NMR (121.4 MHz, C_6D_6): δ −59.2 (s). HRMS and combustion analyses were not successful. This is probably due to oxidation during the measurements. NMR charts are given in Supporting Information of ref.[1a]

Crystal data for **1a**: monoclinic, $P2_1/n$ (#14), a = 6.3438(3) Å, b = 18.0866(5) Å, c = 10.4720(6) Å, β = 100.732(1)°, V = 1180.52(9) Å^3, Z = 4. Data collection: Rigaku RAXIS-RAPID Imaging Plate diffractometer, T = −153 °C. $2\theta_{max}$ = 55.0°, R = 0.041, R_w = 0.076, $I > 1.5\ \sigma(I)$, GOF = 1.96.

1-Boranato-4-phenyl-1-phospha-4-silabicyclo[2.2.2]octane (14).[1a] Mp 136 °C; ^{1}H NMR ($CDCl_3$) δ 1.23−1.32 (m, 6H), 2.16−2.24 (m, 6H), 7.36−7.45 (m, 5H); ^{13}C NMR ($CDCl_3$) δ 3.8 (d, J_{C-P} = 6.3 Hz, 3C), 18.2 (d, J_{C-P} = 34.3 Hz, 3C), 128.2 (2C), 130.4 (1C), 132.8 (d, J_{C-P} = 3.4 Hz, 1C), 133.9 (2C); ^{31}P NMR ($CDCl_3$) δ −8.5 (br d J_{P-B} = 70.2 Hz); HRMS (APCI) calcd for $C_{12}H_{18}PSi$ $(M\text{-}BH_3 + H)^+$ m/z 221.09154. Found m/z 221.09094.

Crystal data for **14**: monoclinic, $P2_1$ (#4), a = 6.3632(3) Å, b = 7.6482(3) Å, c = 13.6844(7) Å, β = 97.056(2)°, V = 660.93(5) Å^3, Z = 2. Data collection: Rigaku RAXIS-RAPID Imaging Plate diffractometer, T = −153 °C. $2\theta_{max}$ = 54.9°, R = 0.028, R_w = 0.037, $I > 1.5\ \sigma(I)$, GOF = 1.26.

***trans*-[RhCl(CO)(Ph-SMAP)$_2$] (17).** To a solution of [{RhCl-$(CO)_2$}$_2$] (58 mg, 0.15 mmol), in C_6H_6 (1.5 mL) was slowly added Ph-SMAP (140 mg, 0.63 mmol) at room temperature and stirred for 1 h. The mixture was concentrated under a reduced pressure. The crude yellow solid was washed with degassed MeOH and hexane. The yellow solid was dissolved in degassed CH_2Cl_2. The solution was transferred to another flask through cannula tube, the inlet of which was covered with a filter paper. Degassed EtOH was carefully added over the CH_2Cl_2 solution. The solution was kept standing at 5 °C. After large yellow crystals were grown, a mother liquor was removed with a syringe. The crystals were dried in vacuo. Mp 183.0−184.2 °C (dec., in a sealed tube). ^{1}H NMR (300 MHz, C_6D_6): δ 0.77−0.83 (m, 12H), 2.44−2.52 (m, 12H), 7.12−7.15 (m, 10H). ^{31}P NMR (121.4 MHz, C_6D_6): δ −8.8 (d, J_{P-Rh} = 117.8 Hz). Anal. Calcd for $C_{25}H_{34}ClOP_2RhSi_2$: C 49.47%, H 5.65%. Found: C 49.20%, H 5.54%. The measurement of ^{13}C NMR was unsuccessful because of the low solubility in C_6D_6 and the reactivity in CD_2Cl_2 at room temperature.

Crystal data for **20**: monoclinic, $P2_1/c$ (#14), a = 6.914(4) Å, b = 6.698(4) Å, c = 28.42(2) Å, β = 95.71(4)°, V = 1309(1) Å^3, Z = 2. Data collection: Rigaku RAXIS-RAPID Imaging Plate diffractometer, T = −163 °C. $2\theta_{max}$ = 55.0°, R = 0.043, R_w = 0.094, $I > 1.5\ \sigma(I)$, GOF = 3.25.

***cis*-[PtMe$_2$(Ph-SMAP)$_2$] (18).** To a C_6D_6 suspension of $[PtMe_2(cod)]$[26] (2.3 mg, 0.007 mmol) in an NMR tube was added Ph-SMAP (3 mg, 0.014 mmol). The mixture was shaken. After 30 min,**18** was given. Sample for X-ray diffraction of **18** was obtained by recrystallization from CH_2Cl_2/hexane. ^{1}H NMR (300 MHz, C_6D_6): δ 1.32−1.50 (dd, J_{H-P} = 6.6 Hz, 7.4 Hz,^{195}Pt satellite J_{H-Pt} = 67.4 Hz, 6H), 2.17−2.21 (m, 12H), 7.15−7.20 (m, 6H), 7.25−7.29 (m, 4H).^{13}C NMR (75.4 MHz, C_6D_6): δ 3.2 (dd, J_{C-P} = 10.0 Hz, 103.4 Hz, ^{195}Pt satellite J_{C-Pt} = 597 Hz, 2C), 5.38−18.0

(26) Clark, H. C.; Manzer, L. E. *J. Organomet. Chem.* **1973**, *59*, 411–428.

(m, 6C), 20.2−20.9 (m, 6C), 128.8 (4C), 130.6 (2C), 134.2 (4C), 135.0 (2C). ^{31}P NMR (121.4 Hz, C_6D_6): δ −21.3 (s, ^{195}Pt satellite J_{P-Pt} = 1785 Hz).

Crystal data for **18**: monoclinic, $P2_1/a$ (#14), a = 11.626(1) Å, b = 18.686(2) Å, c = 14.094 Å, β = 101.368(2)°, V = 3001.9(6) Å^3, Z = 4. Data collection: Rigaku RAXIS-RAPID Imaging Plate diffractometer, T = −150 °C. $2\theta_{max}$ = 55.0°, R = 0.074, R_w = 0.104, $I > 3\ \sigma(I)$, GOF = 3.31.

General Procedure for the Rh-Catalyzed Hydrosilylation of Ketones. In a glovebox, a phosphine (0.01 or 0.02 mmol) and $[\{RhCl(C_2H_4)_2\}_2]$[27] (1.9 mg, 0.005 mmol), and an internal standard (dibenzyl, 45.6 mg, 0.25 mmol) were placed in a vial tube. Anhydrous, degassed benzene (1 mL) was added, and the mixture was stirred at room temperature for a few minutes. Then, Me_2PhSiH (163.5 mg, 1.2 mmol) and a ketone (1.0 mmol) were added. After being sealed with a screw cap, the vial tube was removed from the glovebox. Conversion of the reaction was checked by GLC. After the reaction was completed, the mixture was subjected to column chromatography (SiO_2/Et_2O) and the yields of the products were determined by GC analysis.

General Procedure for the Rh-Catalyzed Hydrogenation of Ketones. In a glovebox, a phosphine (0.01 or 0.02 mmol) and $[Rh(OMe)(cod)]_2$ (2.4 mg, 0.005 mmol) were placed in a screw test tube. A ketone (1.0 mmol) and anhydrous, degassed THF (1 mL) were added. After being sealed with a screw cap, the test tube was removed from the glovebox. The test tube was placed in an autoclave whilebeing flushed with a stream of argon. The autoclave was initially pressurized with hydrogen at 20 atm, before the pressure was reduced to 1 atm by carefully releasing the stop valve. This procedure was repeated three times, and then the vessel was pressurized at 30 atm. The reaction mixture was vigorously stirring at 100 °C. After stirring for 20 h and cooling to room temperature, the hydrogen gas was carefully released. An internal standard ($Cl_2CHCHCl_2$, 20 μL, 0.18 mmol) was added to the reaction mixture. Yield of the product was determined by ^{1}H NMR analysis.

(27) Cramer, R. *Inorg. Synth.* **1990**, *28*, 86–88.

Acknowledgment. This work was supported by the PRESTO program (JST) and by Grant-in-Aid for Scientific Research (B) (No. 18350047) (JSPS). A.O. thanks JSPS for a fellowship. G.H. was supported by MEXT program, Initiatives for Attractive Education in Graduate Schools (T-type Chemists with Lofty Ambition) and GCOE (Catalysis as the Basis for Innovation in Materials Science). We thank Professor T. Inabe (Hokkaido University) for his precious effort in the X-ray structure analyses.

Supporting Information Available: A CIF file for **1a**, **14**, **17**, and **18**·(hexane)$_{0.5}$ and NMR charts for **12** and **13**. This material is available free of charge via the Internet at http://pubs.acs.org.

OM8005728